

# Clustering of Ions at Atomic Dimensions in Quantum Plasmas

P. K. Shukla<sup>1,2</sup> and B. Eliasson<sup>1</sup>

<sup>1</sup>*International Centre for Advances Studies in Physical Sciences & Institute for Theoretical Physics, Faculty of Physics & Astronomy, Ruhr-University Bochum, D-44780 Bochum, Germany*

<sup>2</sup>*Department of Mechanical and Aerospace Engineering & Center for Energy Research, University of California San Diego, La Jolla, CA 92093, U. S. A.\**

(Dated: 22 November 2012)

By means of particle simulations of the equations of motion for ions interacting among themselves under the influence of newly discovered Shukla-Eliasson attractive force (SEAF) in a dense quantum plasma, we demonstrate that the SEAF can bring ions closer at atomic dimensions. We present simulation results of the dynamics of an ensemble of ions in the presence of the SEAF without and with confining external potentials and collisions between the ions and degenerate electrons. Our particle simulations reveal that under the SEAF, ions attract each other, come closer and form ionic clusters in the bath of degenerate electrons that shield the ions. Furthermore, an external confining potential produces robust ion clusters that can have cigar-like and ball-like shapes, which remain stable when the confining potential is removed. The stability of ion clusters is discussed. Our results may have applications to solid density plasmas (density exceeding  $10^{23}$  per cubic centimeters), where the electrons will be degenerate and quantum forces due to the electron recoil effect caused by the overlapping of electron wave functions and electron tunneling through the Bohm potential, electron-exchange and electron-exchange and electron correlations associated with electron-1/2 spin effect, and the quantum statistical pressure of the degenerate electrons play a decisive role.

PACS numbers: 71.10.Ca, 63.10.+a, 67.10.Hk

During the early thirties, there were several discoveries related to non-Coulombic shielded potential distributions that exhibit the role of collective interactions between electrons and ions in electro-chemistry (Debye & Hückel, 1923) (viz. electrolytes and colloidal suspensions), solid state (Fermi, 1927, Thomas, 1927) and gaseous (Langmuir, 1929) plasmas, and between neutrons and protons in elementary particle physics (Yukawa, 1935). The screened non-Coulombic potentials, which were obtained by using linearized theory based on the assumption that the potential energy between the particles is much smaller than the particle kinetic energy, are now known as the Debye-Hückel (DH), Thomas-Fermi (TF), and Yukawa potentials in the context of electro-chemistry and plasma physics, condensed matter physics, and nuclear physics, respectively. The DH, TF, and Yukawa potentials describe short-range (of the order of the DH radius, the TF radius, and the Yukawa radius, which are fixed by the size of a shielded cloud) repulsive interactions between two particles that have the same polarity. The DH theory has also been extended to dusty plasma physics where charged dust particles are shielded by non-degenerate electrons and ions. The DH, TF, and Yukawa interaction potentials, which significantly deviate from the long-range Coulomb interaction potential, have important applications to the understanding of phase transitions (Avinash, 2007, Klumov, 2010, Kremer *et al.*, 1986) in different areas of physical sciences.

In order for charged particles to form ordered struc-

tures under the influence of Coulombic, DH, TF and Yukawa repulsive forces, one must confine the like-charged particles in an external potential, so as to bring them to a minimum energy state. Examples include the Wigner crystals (Wigner, 1934) composed of an ensemble of electrons on the surface of liquid helium, ion crystals in laser cooled Paul (Drewsen *et al.*, 1998) and Penning (electromagnetic) traps (Tan *et al.*, 1995), charged dust particle crystals (Wuerker *et al.*, 1959), which were formed when like-charged dust particles were kept together via external confining potentials despite short-range Coulombic or shielded Coulombic repulsive forces between charged dust particles. In fact, both electron and ion crystals, as well as crystals of colloidal suspensions and oil droplets have been observed experimentally under different physical circumstances (Berg & Gaukler, 1969, Deshpande & Bockrath, 2008, Drewsen *et al.*, 1998, Grimes & Adams, 1979, Mølhave & Drewsen, 2000, Robertson & Younger, 1999, Staannum *et al.*, 2010, Tan *et al.*, 1995, Winter & Ortjohann, 1991). Moreover, an ensemble of strongly correlated micron-sized negative dust particles form dust Coulomb crystals (Barkan & Merlino, 1995, Chu & I, 1994, Fortov *et al.*, 1997, Hayashi & Tachibana, 1994, Mohideen *et al.*, 1998, Thomas *et al.*, 1994) when they were confined by the sheath parabolic potential in low-temperature laboratory dusty plasma discharges (Shukla & Eliasson, 2009, Shukla & Mamun, 2002). The condensation of charged dust particles occurs since the dusty plasma  $\Gamma_d$  (the ratio between the Coulomb energy between highly charged dust grains and the average dust particle kinetic energy) becomes relatively large due to the high dust charge state and low dust temperature. The attraction between like-charged

\*Electronic address: profshukla@yahoo.de

dust particles forming dust Coulomb crystals may also be attributed to attractive forces arising from overlapping of the dusty plasma Debye spheres (Resendes *et al.*, 1998), ion focusing and wakefield effects (Nambu *et al.*, 1995, Shukla & Rao, 1996, Vladimirov & Nambu, 1995), and dust dipole-dipole interactions (Mohideen *et al.*, 1998, Shukla & Eliasson, 2009, Shukla & Mamun, 2002). The Cooper's pairing of charged dust particles, which are glued by ions, led to the discovery of a soft-condensed matter of dust particle crystals in low-density and low-temperature classical plasma with Maxwell-Boltzmann distributions for electrons and ions. It turns out that several milestones were reached in the areas of ordered crystalline structures composed of charged particles (e.g. an ensemble of in low-temperature physical systems electrons, ions, as well as charged colloidal and dust particles) in physical systems, which share some common physics.

However, solid density plasmas are of fundamental importance for industrial applications (e.g. semiconductors, nano-diodes and metallic nanostructures for thin films), for inertial confinement fusion (ICF) schemes that utilizes high density compressed (HDC) plasmas, as well as for planetary systems [e.g. the core of Jupiter (Fortov, 2009)] and superdense astrophysical objects (e.g. the cores of white dwarf stars, warm dense matter). In dense plasmas, one has to account for degeneracy (Chandrasekhar, 1931, 1939) of electrons which obey the Fermi-Dirac distribution function. Correspondingly, quantum mechanical effects play a vital role since in such dense plasmas the Wigner-Seitz radius  $d = (3/4\pi n_0)^{1/3}$  is comparable to the thermal de Broglie wavelength  $\lambda_B = \hbar/mV_T$  (which is a measure of the extent of electron wave functions), where  $\hbar$  is Planck's constant divided by  $2\pi$ ,  $m$  the electron mass,  $V_T = \sqrt{k_B T/m}$  the electron thermal speed due to random electron motions, and  $k_B$  the Boltzmann constant. Also, in dense plasmas with degenerate electrons,  $\lambda_B$  turns out to be much smaller than the Landau length  $\lambda_L = e^2/k_B T$ , which can be conveniently expressed as  $k_B T \ll e^2/a_B$ , where  $a_B = \hbar^2/me^2$  is the Bohr radius of a hydrogen atom. The electron degeneracy effects at nanoscales in dense plasmas can thus be captured through the consideration of the Fermi-Dirac statistics for electrons with spin-1/2 (Fermions), and overlapping of electron wavefunctions due to Heisenberg's uncertainty principle and Pauli's exclusion principle, as well as electron-exchange and electron-correlations. Hence, there are quantum forces (Brodin *et al.*, 2008, Chandrasekhar, 1931, 1939, Crouseilles *et al.*, 2008, Gardner & Ringhofer, 1996, Haas, 2011, Manfredi & Haas, 2001, Manfredi, 2005, Melrose, 2008, Mendonça, 2011, Shaikh & Shukla, 2007, Shukla & Eliasson, 2006, 2007, 2010, 2011, Tsintsadze & Tsintsadze, 2009, Vladimirov & Tyshetskiy, 2011, Wilhelm, 1971) associated with the quantum statistical electron pressure (Chandrasekhar, 1931, 1939, Landau & Lifshitz, 1980), the quantum Bohm potential (Gardner & Ringhofer, 1996, Haas, 2011, Manfredi & Haas, 2001, Manfredi, 2005, Shukla & Eliasson, 2010, 2011, Wil-

helm, 1971) through which degenerate electrons can tunnel through (often known as the quantum electron recoil effect), as well as the electron-exchange and electron-correlations potentials (Brey *et al.*, 1990, Crouseilles *et al.*, 2008, Hedin & Lundqvist, 1971). It has been found that the above mentioned quantum forces acting on degenerate electrons in quantum plasmas introduce new dispersive features to electron plasma oscillations (Bohm, 1952, Bohm & Pines, 1953, Klimontovich & Silin, 1952a,b) with frequencies in the x-ray regime, which can be assessed by using collective x-ray spectroscopic scattering techniques (Glenzer & Redmer, 2009, Glenzer *et al.*, 2007). In fact, Glenzer *et al.* (2007) have reported observations of electron plasma oscillations (EPOs) in warm dense matter (with the peak electron number density  $\sim 3 \times 10^{23} \text{ cm}^{-3}$  and the equilibrium electron and ion temperatures of 12 eV ( $\sim 1.5 \times 10^5$  degrees Kelvin). The latter is different from the electron Fermi temperature  $T_F = (\hbar^2/2k_B m_e)(3\pi^2 n_0)^{2/3} \approx 1.7 \times 10^5$  degrees Kelvin, corresponding to an electron number density  $n_0 \approx 2.5 \times 10^{23} \text{ cm}^{-3}$ ). Thus, the recent experiments of Glenzer *et al.* (2007) have unambiguously demonstrated the importance of the quantum statistical pressure and quantum electron recoil effects on the frequency spectra of EPOs (Bohm, 1952, Bohm & Pines, 1953, Klimontovich & Silin, 1952a,b, Shukla & Eliasson, 2010, 2011), although a previous experimental investigation Watanabe (1956) had already established the quantum dispersion properties of EPOs in metals.

Very recently, Shukla & Eliasson (2012a,b,c) discovered an oscillating shielded Coulomb (OSC) potential, (also referred to as the Shukla-Eliasson attractive potential (SEAP) (Akbari-Moghanjoughi, 2012)), which is valid for the potential energy much smaller than  $k_B T$  and  $mc^2$ , around a stationary test ion in an unmagnetized quantum plasma, where  $c$  is the speed of light in vacuum. The SEAP arises due to collective interactions between an ensemble of degenerate electrons that shield an isolated ion at atomic dimensions. The profile of the SEAP in quantum plasmas resembles the Lennard-Jones (LJ) potential in atomic gases. The Shukla-Eliasson attractive force (SEAF), defined as minus the gradient of the SEAP, brings ions closer to form ion clusters in quantum plasmas. In this paper, we demonstrate the formation of ion clusters at atomic dimensions by performing computer simulations of the equations of motion for an ensemble of ions that are interacting with each other through the SEAF.

## I. THE SEAF

The existence of the SEAP, which is obtained from Fourier transformation of Poisson's equation with the quasi-stationary electron density perturbation deduced from the linearized continuity and generalized momentum equation (Shukla & Eliasson, 2012a,b,c) for non-relativistic, degenerate electrons in a dense quan-

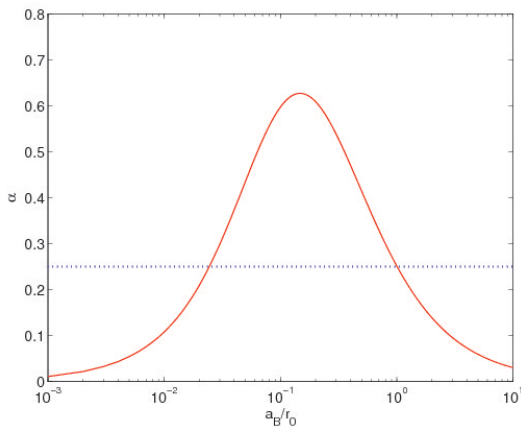


FIG. 1: The value of  $\alpha$  as a function of  $a_B/r_0$ . The critical value  $\alpha = 1/4$  is indicated with a dotted line.

tum plasma, critically depends on the electron number density through the parameter  $\alpha = \hbar^2 \omega_{pe}^2 / 4m^2 u_*^4$ , where  $u_* = (v_*^2/3 + v_{ex}^2)^{1/2}$ . The parameter  $\alpha$  measures the quantum electron recoil effect caused by the quantum Bohm potential (Gardner & Ringhofer, 1996, Manfredi & Haas, 2001, Manfredi, 2005, Wilhelm, 1971)  $V_B = (\hbar^2/2m)(1/\sqrt{n})\nabla^2\sqrt{n}$  compared to the quantum statistical Fermi electron pressure and the electron-exchange and electron-correlation effects arising from 1/2-spin of the degenerate electrons. Here  $v_* = \hbar(3\pi^2)^{1/3}/mr_0$  is the electron Fermi speed and  $v_{ex} = (0.328e^2/mr_0)^{1/2}[1 + 0.62/(1 + 18.36a_B n_0^{1/3})]^{1/2}$  includes the effects of electron exchange and electron correlations, where  $r_0 = n_0^{-1/3}$  represents the average inter-electron distance. The expression for  $v_{ex}$  is derived by linearizing the sum of the electron exchange and electron correlation potentials (Brey *et al.*, 1990, Hedin & Lundqvist, 1971)  $V_{xc} = 0.985e^2 n^{1/3} [1 + (0.034/a_B n^{1/3})\ln(1 + 18.37a_B n^{1/3})]$ . We note that  $\alpha$  depends only on  $a_B/r_0$ , as  $\alpha \simeq 9.3\pi(a_B/r_0)/[1 + (3\pi^2)^{2/3}(a_B/r_0) + 0.62/(1 + 18.36a_B/r_0)]^2$ . Shukla & Eliasson (2012a,b,c) found that attractive potentials between ions exist only for  $\alpha > 1/4$ . Figure 1 displays the value of  $\alpha$  as a function of  $a_B/r_0$ , where one observes that it is above a critical value 0.25 only for a limited range  $2 \times 10^{-2} < a_B/r_0 < 1$ , corresponding to an electron number density in the range  $5.4 \times 10^{19} \text{ cm}^{-3} < n_0 < 6.7 \times 10^{24} \text{ cm}^{-3}$  (with  $a_B = 5.3 \times 10^{-9} \text{ cm}$ ). The maximum value is  $\alpha \approx 0.627$  at  $a_B/r_0 \approx 0.15$ , corresponding to the electron number density  $n_0 \approx 2 \times 10^{22} \text{ cm}^{-3}$ , a few times below solid densities. The validity of the SEAP has been further expanded (Akbari-Moghanjoughi, 2012) for wider density ranges by including Chandrasekhar's (1931, 1939) generalized pressure law for degenerate electron fluids and Salpeter's (1961) electron-exchange and electron-correlation potentials that are of astrophysical interest (e.g. the cores of white dwarf stars). The nonlinear shielding effects on the SEAF is discussed by Shukla *et*

*al.* (2012).

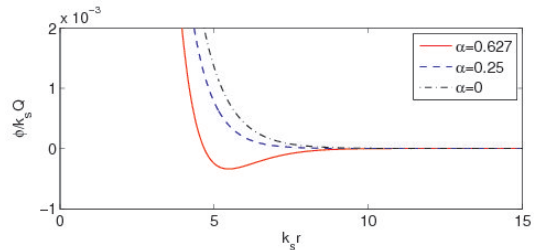


FIG. 2: (Color online) The electric potential  $\phi$  as a function of  $r$  for  $\alpha = 0.627$  (solid curve),  $\alpha = 0.25$  (dashed curve) and  $\alpha = 0$  (dash-dotted curve). The value 0.627 is the maximum possible value of  $\alpha$  in our model, obtained for  $a_B/r_0 \approx 0.15$ .

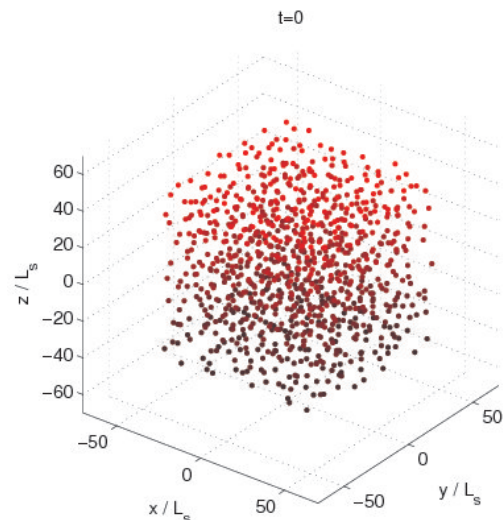


FIG. 3: (Color online) The initial positions of ions in the particle simulations.

For  $\alpha > 0.25$ , the profile of the electric potential as a function of distance  $r$  around a stationary test ion charge  $Q$  is (Shukla & Eliasson, 2012a,b,c)

$$\phi(\mathbf{r}) = \frac{Q}{r} [\cos(k_i r) + b_* \sin(k_i r)] \exp(-k_r r), \quad (1)$$

which is referred to as the SEAP. Here  $Q$  is the ion charge,  $b_* = 1/\sqrt{4\alpha - 1}$ ,  $k_i = (k_s/\sqrt{4\alpha})(\sqrt{4\alpha} - 1)^{1/2}$ , and  $k_r = (k_s/\sqrt{4\alpha})(\sqrt{4\alpha} + 1)^{1/2}$ , with  $k_s = \omega_{pe}/u_*$  being the modified inverse TF screening length. The spatial profile of the SEAP in Fig. 2 shows a distinct minimum for the case  $\alpha = 0.627$ . The negative part of the SEAP, given by Eq. (1), resembles the LJ potential and leads to a short-range SEAF between neighboring ions. On the other hand, the potential distribution around a test ion for  $\alpha < 0.25$  reads (Shukla & Eliasson, 2012a,b,c)

$$\phi(\mathbf{r}) = \frac{Q}{2r} [(1 + b) \exp(-k_+ r) + (1 - b) \exp(-k_- r)], \quad (2)$$

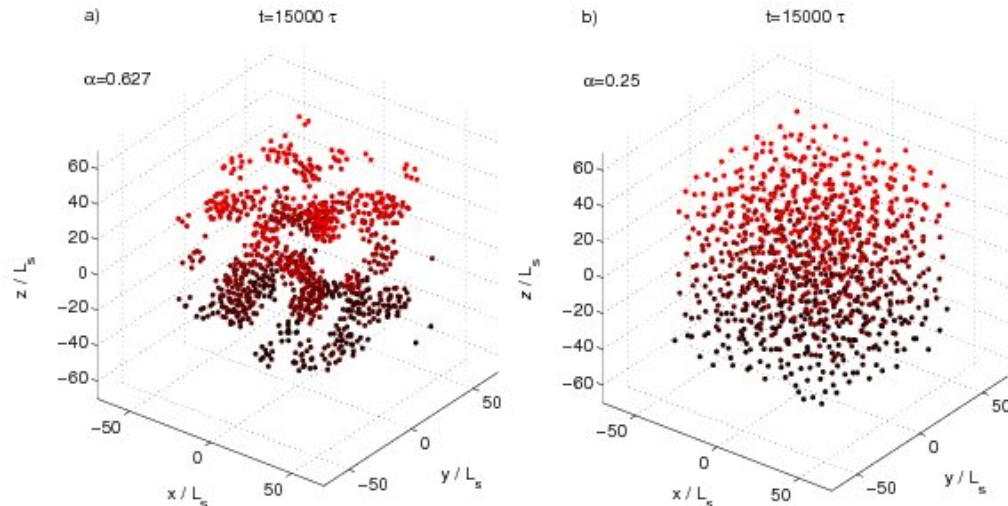


FIG. 4: (Color online) The positions of ions  $t = 15000$  for a)  $\alpha = 0.627$  and b)  $\alpha = 0.25$ , showing the clustering and solidification of ions for  $\alpha = 0.627$ , but not for  $\alpha = 0.25$ .

where  $b = 1/\sqrt{1-4\alpha}$ , and  $k_{\pm} = k_s(1 \mp \sqrt{1-4\alpha})^{1/2}/\sqrt{2\alpha}$ . For this case, the potential is positive and monotonically decreasing (cf. Fig. 2), giving rise to only a repulsive force (similar to the TF force) between ions. In the high- or low-density limit, where  $\alpha \rightarrow 0$ , we recover the modified TF screened Coulomb potential  $\phi(\mathbf{r}) = (Q/r)\exp(-k_s r)$ .

## II. DEMONSTRATION OF ION CLUSTERING

We here present a computer simulation study of the dynamics of a system of ions interacting with each other under the action of the SEAF. For this purpose, we numerically solve the equations of motion for a system of ions with equal charges and masses, given by

$$M \frac{d\mathbf{v}_j}{dt} = -Q \sum_{i \neq j} \nabla_j \phi(|\mathbf{R}_{ij}|) - \nabla_j V_c(\mathbf{r}_j) - M\nu \mathbf{v}_j, \quad (3)$$

where instantaneous position of each ion is determined from  $d\mathbf{r}_j/dt = \mathbf{v}_j$ . Here  $\mathbf{R}_{ij} = \mathbf{r}_i - \mathbf{r}_j$  is the radius vector between particle  $i$  and  $j$ ,  $\mathbf{r}_j(t)$  the position and  $\mathbf{v}_j(t)$  the velocity of the  $j$ th ion,  $M$  the ion mass,  $\nabla_j$  denotes the gradient of  $\phi$  at position  $\mathbf{r}_j$ , and  $\nu$  denotes an effective collision frequency, which tends to retard the ion motion. The external confining potential,  $V_c(\mathbf{r}) = (M/2)(\omega_{\perp}^2 r_{\perp}^2 + \omega_z^2 z^2)$ , of charged particles may have different amplitudes  $\omega_{\perp}$  and  $\omega_z$  perpendicular and parallel to the  $z$ -axis, respectively, where  $r_{\perp}^2 = r_x^2 + r_y^2$ .

In order to demonstrate the clustering of ions under the SEAF, we now carry out particle simulations of Eq. (3) with 1000 particles, initially randomly placed in space, as shown in Fig. 3. In the first set of simulations, displayed in Fig. 4, we consider interactions of the ions in the absence of the external confining potential  $V_c$ , viz.  $\omega_z = \omega_{\perp} = 0$ , and with  $\nu = 0.01 \tau^{-1}$ .

The positions of ions at the end of the simulations are shown in Fig. 4 at time  $t = 15000 \tau$ . Here the positions and time are in units of  $L_s = k_s^{-1}$  and  $\tau = M^{1/2}/Qk_s^{3/2} = (\pi/16)^{1/8}(a_B/r_0)^{3/8}\omega_{pi}^{-1}/\alpha^{3/8}Z_i$ , respectively, where  $\omega_{pi} = (4\pi Q^2 n_{i0}/M)^{1/2}$  is the ion plasma frequency, and  $n_{i0}$  the equilibrium ion number density, related to the electron number density  $n_0$  via the quasi-neutrality condition  $Z_i n_{i0} = n_0$ , where  $Z_i$  is the ion charge state. For  $\alpha = 0.627$ , which leads to a potential minimum (cf. Fig. 2), we observe the clustering of ions and the formation of large-scale ionic structures. The clustering of ions is a relatively slow process in comparison with the ion plasma period  $2\pi/\omega_{pi}$ . Ion pairs and smaller clusters are initially formed, and later the larger ion clusters are gradually formed by the agglomeration of smaller ion clusters. As a contrast, for  $\alpha = 0.25$ , we see in Fig. 4 that there does not exist condensation/coalescence of ions. This is due to the fact that there is no potential minimum for this value of  $\alpha$  (cf. Fig. 2), and hence the inter-ion force is always repulsive for this case.

Furthermore, we have carried out a set of simulations with a symmetric potential  $V_c$  with  $\omega_{\perp} = \omega_z = 2 \times 10^{-3} \tau^{-1}$ . Here, as seen in Fig. 5, almost spherical non-Coulombic ion crystals are formed for both  $\alpha = 0.627$  and  $\alpha = 0.25$ . We also performed simulations including an asymmetric external potential  $V_c$  with  $\omega_{\perp} = 6 \times 10^{-3} \tau^{-1}$  and  $\omega_z = 2 \times 10^{-3} \tau^{-1}$ , providing a stronger confinement in the perpendicular direction. Figure 6 displays the final state for  $\alpha = 0.627$  and  $\alpha = 0.25$ , where ions, in both cases, form non-Coulombic ion crystals elongated along the  $z$ -direction. In general, the formation of non-Coulombic ion crystals is attributed to the balance between the external and inter-ion potentials, where the system tends to a configuration of a minimum potential energy. We note that similar configurations have been previously reported for both charged

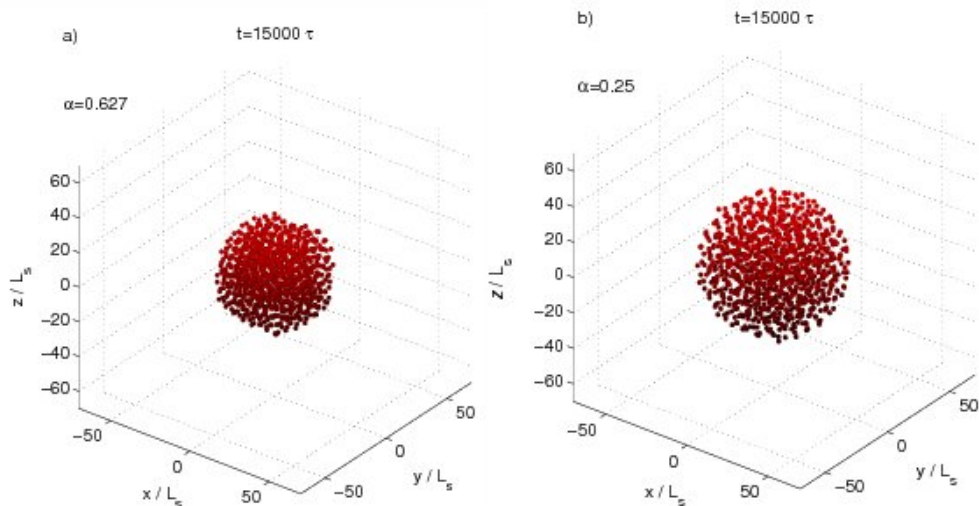


FIG. 5: (Color online) The positions of ions at  $t = 15000$  for a)  $\alpha = 0.627$  and b)  $\alpha = 0.25$  including a symmetric parabolic potential with  $\omega_{\perp} = \omega_z = 2 \times 10^{-3} \tau^{-1}$ . Almost spherical non-Coulombic ion crystals are formed.

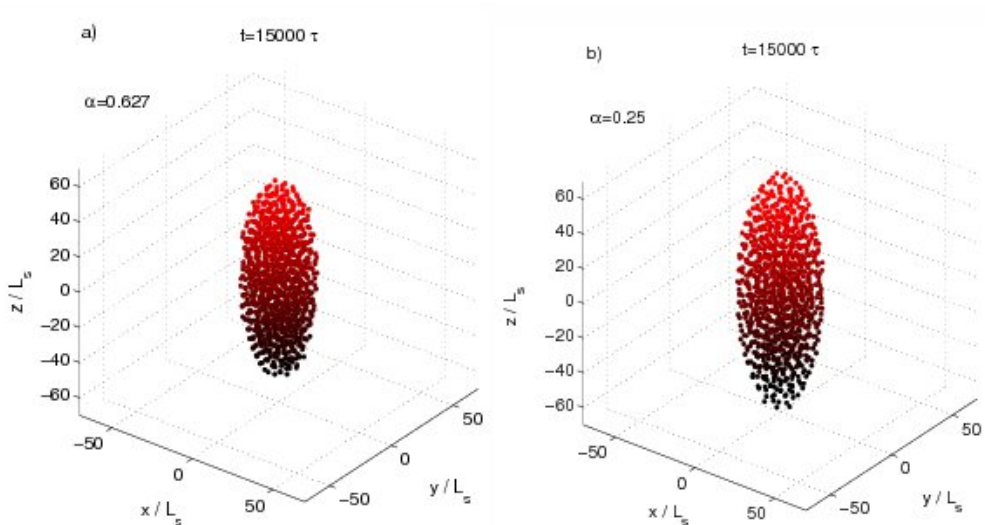


FIG. 6: (Color online) The positions of ions at  $t = 15000$  for a)  $\alpha = 0.627$  and b)  $\alpha = 0.25$  including an asymmetric parabolic potential with  $\omega_{\perp} = 6 \times 10^{-3} \tau^{-1}$  and  $\omega_z = 2 \times 10^{-3} \tau^{-1}$ . Here elongated non-Coulombic ion crystals are formed.

macro-particles (Wuerker *et al.*, 1959) and ions (Drewsen *et al.*, 1998, Mølhave & Drewsen, 2000, Staantum *et al.*, 2010) confined by external potentials in the Paul trap. Finally, in Figs. 7 and 8, we continued the simulations in Figs. 5 and 6 and set the external confining potential to zero at time  $t = 15000\tau$ . For both cases, with symmetric and asymmetric potentials, we see that ion crystals remained tightly packed for  $\alpha = 0.627$ , where it performed damped oscillations as elastic solids before settling down to the final states in Figs. 7(a) and 8(a). In contrast, for  $\alpha = 0.25$ , the ion cloud expanded to larger and less dense ion clouds, as seen in Figs 7(b) and 8(b) at  $t = 20000\tau$ . Hence the short-range potential around ions for  $\alpha = 0.627$  (cf. Fig. 2) lead to the solidification of the ions, which is not the case for the the short-range

repulsive potential for  $\alpha = 0.25$ .

### III. SUMMARY AND CONCLUSIONS

In this paper, we have carried out particle simulations to demonstrate clustering of ions due to the newly found SEAF arising from collective interactions between an ensemble of degenerate electrons that shield ions in dense quantum plasmas. Specifically, the SEAF leads to clustering/condensation or coagulation of ions in the absence of an external confining potential for charged particles. However, ion clustering can be put on the firm footing by calculating the dynamical ion structure factor (DISF) based on the fluctuation-dissipation theorem and the di-



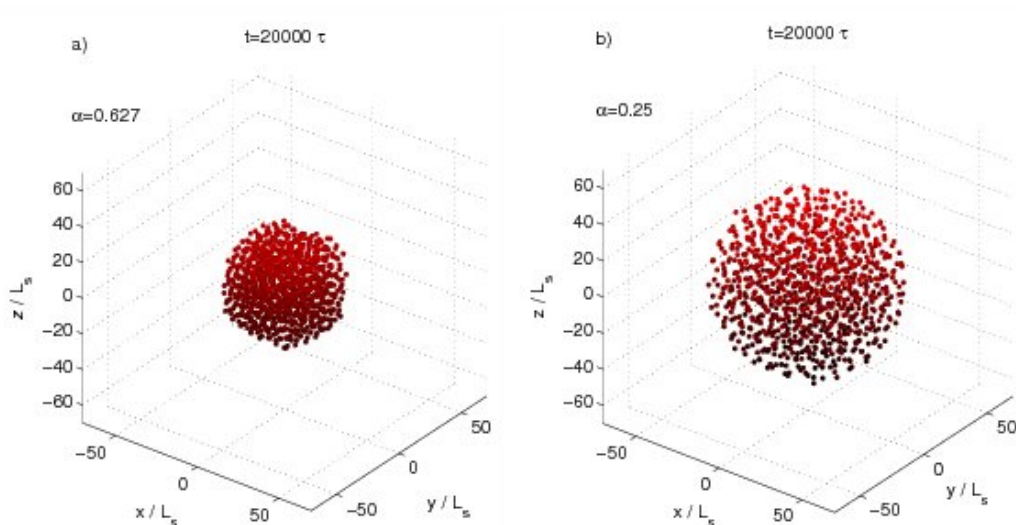


FIG. 7: (Color online) The positions of ions at  $t = 20000\tau$  for a)  $\alpha = 0.627$  and b)  $\alpha = 0.25$  for the case of a symmetric parabolic potential in Fig. 5, where the potential is set to zero at  $t = 15000\tau$ . The ion cluster remains tightly packed for  $\alpha = 0.627$ , while the ion cloud expands for  $\alpha = 0.25$ .

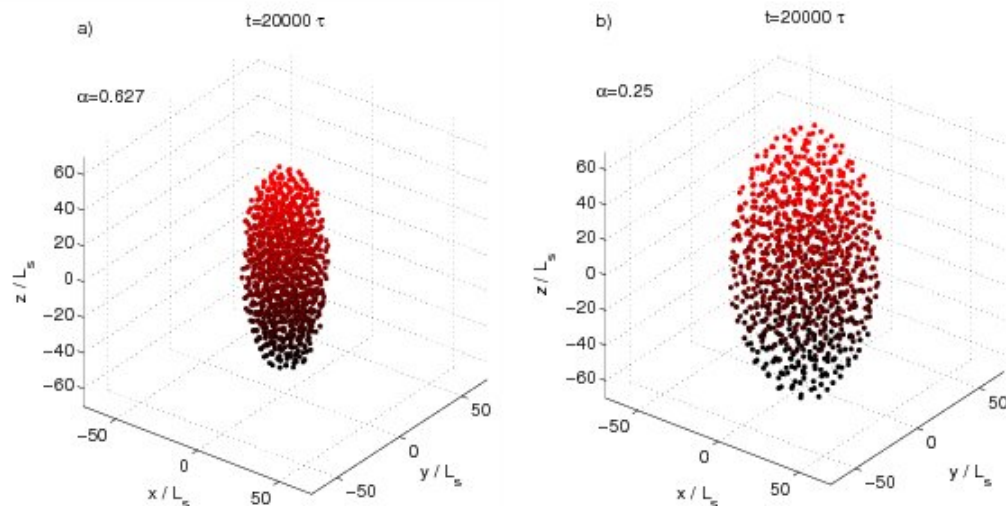


FIG. 8: (Color online) The positions of ions at  $t = 20000\tau$  for a)  $\alpha = 0.627$  and b)  $\alpha = 0.25$  for the case of an asymmetric parabolic potential in Fig. 6, where the potential is set to zero at  $t = 15000\tau$ . The ion cluster remains tightly packed for  $\alpha = 0.627$ , while the ion cloud expands for  $\alpha = 0.25$ .

electric constant of degenerate electrons and strongly correlated ions in a viscous quantum plasma. It may well turn out that the DISF will reveal long-range correlations between ions. It is our belief that the formation of ion nano-clusters is going to play a valuable role in the area of high-density compressed plasmas with degenerate electrons (Glenzer & Redmer, 2009, Malkin *et al.*, 2007, Son & Fisch, 2004, 2005, 2006) for ICF to succeed, and also in the emerging field of nano-material sciences (e.g. nanodiods, metallic nanostructures for thin films (Crouseilles *et al.*, 2008), nanowires), where closely-packed ions will lend support to enhanced fusion probabilities (with anomalous fusion cross-sections) for controlled thermonuclear

ICF, and may also influence the electric properties (e.g. resistivity) of new high density plasma materials at relatively high temperatures. Finally, we stress that the Cooper pairing of ions at atomic dimensions shall provide possibility of novel superconducting plasma-based nanotechnology, since the electron transport in nanostructures would be rapid due to shortened distances between ions in the presence of the novel SEAF.

## Acknowledgments

This work was supported by the Deutsche Forschungsgemeinschaft through the project SH21/3-2 of the Re-

search Unit 1048.

- Akbari-Moghanjoughi, M. 2012 Shukla-Eliasson attractive force: revisited. *J. Plasma Phys.* **78**, in press; DOI: <http://dx.doi.org/S00223778120000839>; E-print: arXiv:1207.5154v2 [astro-ph.EP].
- Avinash, K. 2007 Mean-field theory of critical phenomenon for mutually repelling particles in complex plasmas. *Phys. Rev. Lett.* **98**, 095003.
- Barkan, A. & Merlino, R. L. 1995 Confinement of dust particles in a double layer. *Phys. Plasmas* **2**, 3261–3265.
- Berg, T. G. O. & Gaukler, T. A. 1969 Apparatus for the study of charged particles and droplets. *Am. J. Phys.* **37**, 1013–1018.
- Bohm, D. 1952 A suggested interpretation of the quantum theory in terms of "hidden" variables. I. *Phys. Rev.* **85**, 166–179.
- Bohm, D. & Pines, D. 1953 A collective description of electron interactions: III. Coulomb interactions in a degenerate electron gas. *Phys. Rev.* **92**, 609–625.
- Brey, L., Dempsey, J., Johnson, N. F. & Halperin, B. I. 1990 Infrared optical absorption in imperfect parabolic quantum wells. *Phys. Rev. B* **42**, 1240–1247.
- Brodin, G., Marklund, M. & Manfredi, G. 2008 Quantum plasma effects in the classical regime. *Phys. Rev. Lett.* **100**, 175001.
- Chandrasekhar, S. 1931 The maximum mass of ideal white dwarfs. *Astrophys. J.* **74**, 81–82.
- Chandrasekhar, S. 1939 *An Introduction to the Study of Stellar Structure* (The University of Chicago Press, Chicago).
- Chu, J. H. & I, L. 1994 Direct Observation of Coulomb crystals and liquids in strongly coupled rf dusty plasmas. *Phys. Rev. Lett.* **72**, 4009–4012.
- Crandall, R. S. & Williams, R. 1971 Crystallization of electrons on the surface of liquid helium. *Phys. Lett. A* **34**, 404–405.
- Crouseilles, N., Hervieux, P. A. & Manfredi, G. 2008 Quantum hydrodynamic model for the nonlinear electron dynamics in thin metal films. *Phys. Rev. B* **78**, 155412.
- Debye, P., & Hückel, E. 1923 Zur Theorie der Electrolyte I. Gefrierpunktserniedrigung und verwandte Erscheinungen. *Phys. Z.* **24**, 185–206.
- Deshpande, V. V., & Bockrath, M. 2008 The one-dimensional Wigner crystal in carbon nanotubes. *Nature Phys.* **4**, 314–318.
- Drewsen, M., Brodersen, C., Hornekær, L., Hangst, J. S., & Schiffer, J. P. 1998 Large ion crystals in a linear Paul trap. *Phys. Rev. Lett.* **81**, 2878–2881.
- Fermi, E. 1927 Un metodo statistico per la determinazione di alcune proprietà dell'atomo. *Rend. Acad. Na. Lincei* **6**, 602–607.
- Fortov, V. E. 2009 Extreme state of matter on earth and in space. *Phys. Usp.* **52**, 615–647.
- Fortov V. E., Nefedov, A. P., Torchinsky, V. M., Molotkov, V. I., Petrov, O. F., Samarian, A. A., Lipaev, A. A. & Khrapak, A. G., Crystalline structure of strongly coupled dusty plasmas in dc glow discharge strata, *Phys. Lett. A* **229**, 317–322.
- Gardner, C. L. & Ringhofer, C. 1996 Smooth quantum potential for the hydrodynamic model. *Phys. Rev. E* **53**, 157–167.
- Glenzer S. H. & Redmer, R. 2009 X-ray Thomson scattering in high energy density plasmas. *Rev. Mod. Phys.* **81**, 1625–1663.
- Glenzer, S. H., Landen, O. L., Neumayer, P., Lee, R. W., Widmann, K., Pollaine, S. W., Wallace, R. J., Gregori, G., Holl, A., Bornath, T., Thiele, R., Schwarz, V., Kraeft, W. D., Redmer, R. 2007 Observations of plasmons in warm dense matter. *Phys. Rev. Lett.* **98**, 065002.
- Grimes, C. C. & Adams, G. 1979 Evidence for a liquid-to-crystal phase transition in a classical, two-dimensional sheet of electrons, *Phys. Rev. Lett.* **42**, 795–798.
- Haas, F. 2011 *Quantum Plasmas: An Hydrodynamical Approach* (Springer, New York).
- Hayashi, Y. & Tachibana, K. 1994 Observation of Coulomb-crystal formation from carbon particles grown in a methane plasma. *Jpn. J. Appl. Phys.* **33**, L804–L806.
- Hedin, L. & Lundqvist, B. I. 1971 Explicit local exchange-correlation potentials. *J. Phys. C: Solid State Phys.* **4**, 2064–2083.
- Klimontovich, Yu. L. & Silin, V. P. 1952a *Dokl. Akad. Nauk SSSR*, **82**, 361.
- Klimontovich, Yu. L. & Silin, V. P. 1952b Concerning the spectra of systems of interacting particles. *Zh. Eksp. Teor. Fiz.* **23**, 151–160.
- Klumov, B. 2010 On melting criteria for complex plasma. *Phys. Usp.* **53**, 1053–1065.
- Kremer, K., Robbins, M. O., & Grest, G. S. 1986 Phase diagram of Yukawa systems: Model for charge-stabilized colloids. *Phys. Rev. Lett.* **57**, 2694–2697.
- Landau, L. D. & Lifshitz, E. M. 1980 *Statistical Physics* (Butterworth-Heinemann, Oxford).
- Langmuir, I. 1929 The interaction of electron and positive ion space charges in cathode sheaths. *Phys. Rev.* **33**, 954–989.
- Malkin, V. M., Fisch, N. J., & Wurtele, J. S. 2007 Compression of powerful x-ray pulses to attosecond durations by stimulated Raman backscattering in plasmas. *Phys. Rev. E* **75**, 026404.
- Manfredi, G. & Haas, F. 2001 Self-consistent fluid model for a quantum electron gas. *Phys. Rev. B* **64**, 075316.
- Manfredi, G. 2005 How to model quantum plasmas. *Fields Inst. Commun.* **46**, 263–287.
- Melrose, D. B. 2008 *Quantum Plasmadynamics: Unmagnetized Plasmas* (Springer, Berlin).
- Mendonça, J. T. 2011 Wave kinetics of relativistic quantum plasmas. *Phys. Plasmas* **18**, 062101.
- Mohideen, U., Rahman, H. U., Smith, M. A., Rosenberg, M., & Mendis, D. A. 1998 Intergrain coupling in dusty-plasma Coulomb crystals. *Phys. Rev. Lett.* **81**, 349–352.
- Mølhave, K. & Drewsen, M. 2000 Formation of translationally cold MgH<sup>+</sup> and MgD<sup>+</sup> molecules in an ion trap. *Phys. Rev. A* **62**, 011401.
- Nambu, M., Vladimirov, S. V., & Shukla, P. K. 1995 Attractive forces between charged particulates in plasmas. *Phys. Lett. A* **203**, 40–42.

- Resendes, D. F., Mendonça, J. T., & Shukla, P. K. 1998 Formation of dusty plasma molecules. *Phys. Lett. A* **239**, 181–186.
- Robertson, S. & Younger, R. 1999 Coulomb crystals of oil droplets. *Am. J. Phys.* **67**, 310–315.
- Salpeter, E. E. 1961 Energy and Pressure of a Zero-Temperature Plasma. *Astrophys. J.* **134**, 669–682.
- Shaikh D. & Shukla, P. K. 2007 Fluid turbulence in quantum plasmas. *Phys. Rev. Lett.* **99**, 125002.
- Shukla, P. K. & Eliasson, B. 2006 Formation and dynamics of dark solitons and vortices in quantum electron plasmas. *Phys. Rev. Lett.* **96**, 245001.
- Shukla, P. K. & Eliasson, B. 2007 Nonlinear interactions between electromagnetic waves and electron plasma oscillations in quantum plasmas *Phys. Rev. Lett.* **99**, 096401.
- Shukla, P. K. & Eliasson, B. 2009 Fundamentals of dust plasma interactions *Rev. Mod. Phys.* **81**, 25–50.
- Shukla, P. K. & Eliasson, B. 2010 Nonlinear aspects of quantum plasma physics. *Phys. Usp.* **53**, 51–76.
- Shukla, P. K. & Eliasson, B. 2011 Nonlinear collective interactions in quantum plasmas with degenerate electron fluids. *Rev. Mod. Phys.* **83**, 885–906.
- Shukla, P. K. & Eliasson B. 2012a Novel attractive force between ions in quantum Plasmas. *Phys. Rev. Lett.* **108**, 165007.
- Shukla, P. K. & Eliasson B. 2012b Erratum: Novel attractive force between ions in quantum plasmas [Phys. Rev. Lett. 108, 165007 (2012)]. *Phys. Rev. Lett.* **108**, 219902(E).
- Shukla, P. K. & Eliasson B. 2012c Erratum: Novel attractive force between ions in quantum plasmas [Phys. Rev. Lett. 108, 165007 (2012)]. *Phys. Rev. Lett.* **109**, 019901(E).
- Shukla, P. K., Akbari-Moghanjoughi, M. & Eliasson B. 2012 Comment on "On 'Novel attractive forces' between ions in quantum plasmas – failure of linearized quantum hydrodynamics" *arXiv:1206.3456 [physics.plasm-ph]*.
- Shukla, P. K. & Mamun, A. A. 2002 *Introduction to Dusty Plasma Physics* (Institute of Physics, Bristol).
- Shukla, P. K. & Rao, N. N. 1996 Coulomb crystallization in colloidal plasmas with streaming ions and dust grains. *Phys. Plasmas* **3**, 1770–1772.
- Son S. & Fisch, N. J. 2004 Aneutronic fusion in a degenerate plasma. *Phys. Lett. A* **329**, 76–82.
- Son S. & Fisch, N. J. 2005 Current-drive efficiency in a degenerate plasma. *Phys. Rev. Lett.* **95**, 225002.
- Son S. & Fisch, N. J. 2006 Controlled fusion with hot-ion mode in a degenerate plasma. *Phys. Lett. A* **356**, 65–71.
- Staanum, P. F., Højbjerg, K., Skyt, P. S., Hansen A. K. & Drewsen, M. 2010 Rotational laser cooling of vibrationally and translationally cold molecular ions. *Nature Phys.* **6**, 271–274.
- Tan, J. N., Bollinger, J. J., Jelenkovic, B. & Wineland, D. J. 1995 Long-range order in laser-cooled, atomic-ion Wigner crystals observed by Bragg scattering. *Phys. Rev. Lett.* **75**, 4198–4201.
- Thomas, H., Morfill, G. E., Demmel, V., Goree, J., Feuerbacher, B. & Möhlmann, D. 1994 Plasma crystal: Coulomb crystallization in a dusty plasma. *Phys. Rev. Lett.* **73**, 652–655.
- Thomas, L. H. 1927 The calculation of atomic fields. *Math. Proc. Cambridge Phil. Soc.* **23**, 542–548.
- Tsintsadze, N. L. & Tsintsadze, L. N. 2009 Novel quantum kinetic equations of the Fermi particles. *Europhys. Lett.* **88**, 35001.
- Vladimirov, S. V. & Nambu, M. 1995 Attraction of charged particulates in plasmas with finite flows. *Phys. Rev. E* **52**, R2172–R2174.
- Vladimirov, S. V. & Tyshetskiy, Yu. O. 2011 On description of a collisionless quantum plasma. *Phys. Usp.* **54**, 1243–1256.
- Watanabe, H. 1956 Experimental Evidence for the Collective Nature of the Characteristic Energy Loss of Electrons in Solids—Studies on the Dispersion Relation of Plasma Frequency—. *J. Phys. Soc. Jpn.* **11**, 112–119.
- Wigner, E. 1934 On the interaction of electrons in metals. *Phys. Rev.* **46**, 1002–1011.
- Wilhelm, H. E. 1971 Wave-mechanical formulation of plasma dynamics in longitudinal electric fields. *Z. Phys.* **241**, 1–8.
- Winter H. & Ortjohann, H. W. 1991 Simple demonstration of storing macroscopic particles in a "Paul trap". *Am. J. Phys.* **59**, 807–813.
- Wuerker, R. F., Shelton, H. & Langmuir, R. V. 1959 Electrodynamic containment of charged particles. *J. Appl. Phys.* **30**, 342–349.
- Yukawa H. 1935 On the interaction of elementary particles I. *Proc. Phys.-Math. Jpn.* **17**, 48–57.